



Comparison of simultaneous arterial spin labeling MRI and $^{15}\text{O}\text{-H}_2\text{O}$ PET measurements of regional cerebral blood flow in rest and altered perfusion states

Oriol Puig , Otto M Henriksen, Mark B Vestergaard, Adam E Hansen, Flemming L Andersen, Claes N Ladefoged, Egill Rostrup, Henrik BW Larsson, Ulrich Lindberg* and Ian Law*

Abstract

Arterial spin labelling (ASL) is a non-invasive magnetic resonance imaging (MRI) technique that may provide fully quantitative regional cerebral blood flow (rCBF) images. However, before its application in clinical routine, ASL needs to be validated against the clinical gold standard, $^{15}\text{O}\text{-H}_2\text{O}$ positron emission tomography (PET). We aimed to compare the two techniques by performing simultaneous ASL-MRI and $^{15}\text{O}\text{-H}_2\text{O}\text{-PET}$ examinations in a hybrid PET/MRI scanner. Duplicate rCBF measurements were performed in healthy young subjects ($n = 14$) in rest, during hyperventilation, and after acetazolamide (post-ACZ), yielding 63 combined PET/MRI datasets in total. Average global CBF by ASL-MRI and $^{15}\text{O}\text{-H}_2\text{O}\text{-PET}$ was not significantly different in any state (40.0 ± 6.5 and 40.6 ± 4.1 mL/100 g/min, respectively in rest, 24.5 ± 5.1 and 23.4 ± 4.8 mL/100 g/min, respectively, during hyperventilation, and 59.1 ± 10.4 and 64.7 ± 10.0 mL/100 g/min, respectively, post-ACZ). Overall, strong correlation between the two methods was found across all states (slope = 1.01, $R^2 = 0.82$), while the correlations within individual states and of reactivity measures were weaker, in particular in rest ($R^2 = 0.05$, $p = 0.03$). Regional distribution was similar, although ASL yielded higher perfusion and absolute reactivity in highly vascularized areas. In conclusion, ASL-MRI and $^{15}\text{O}\text{-H}_2\text{O}\text{-PET}$ measurements of rCBF are highly correlated across different perfusion states, but with variable correlation within and between hemodynamic states, and systematic differences in regional distribution.

Keywords

Arterial spin labeling, cerebral blood flow, $^{15}\text{O}\text{-H}_2\text{O}\text{-PET}$, perfusion, PET/MRI

Received 5 February 2019; Revised 16 May 2019; Accepted 4 August 2019

Introduction

Positron emission tomography (PET) with ^{15}O -labelled water ($^{15}\text{O}\text{-H}_2\text{O}$) for measurement of regional cerebral blood flow (rCBF) is a well-established technique and often considered the reference method for absolute quantitative physiological measurements.¹ In over 30 years of research, $^{15}\text{O}\text{-H}_2\text{O}$ PET has proven its usefulness in physiologic experiments and for clinical investigational purposes.^{2,3} It is, however, a costly, technically demanding and invasive technique, only accessible in highly specialized centers. Although still a magnetic resonance imaging (MRI) technique under development, arterial spin labeling (ASL), could provide radiation-free, quantitative and non-invasive rCBF imaging.

ASL has been used in the study of brain physiology and can, under optimal conditions, provide results of global (gCBF) and regional CBF comparable to those of the generally accepted reference methods⁴ and has been reported to provide clinically relevant information

Department of Clinical Physiology, Nuclear Medicine and PET, Rigshospitalet, Copenhagen, Denmark

*These authors contributed equally to this work and share senior authorship.

Corresponding author:

Oriol Puig, Department of Clinical Physiology, Nuclear Medicine and PET, Rigshospitalet, Blegdamsvej 9, Copenhagen 2100, Denmark.
Email: oriol.puig.calvo@regionh.dk

in the study of dementias,⁵ epilepsy⁶ and cerebrovascular diseases.⁷

Over the past 10 years, a number of studies have compared the two techniques in healthy and diseased individuals using a range of ASL techniques.^{8–17} The quantitative correlation varies substantially and appears to decrease with the time interval between sequential PET and MRI scan sessions as described in a recent systematic revision analyzing the existing literature comparing the two techniques.¹⁸ The introduction of commercial hybrid PET/MRI scanners has enabled simultaneous ¹⁵O-H₂O PET and ASL MRI measurements under identical conditions, thereby abolishing key sources of physiological variability in the comparison during rest and acutely altered physiological states. However, in our experience, even after implementing and testing a sufficiently robust ASL sequence and post-processing pipeline, the added complexity of simultaneity and the physical constraints of the PET/MRI scanner environment itself may inhibit effective use of this advantage.^{19,20} Thus, previous studies comparing simultaneously acquired ASL MRI and ¹⁵O-H₂O PET have been published up to date are scarce. Zhang et al.⁸ compared resting CBF in healthy individuals using rCBF maps obtained by ASL scaled by global CBF measured by phase contrast mapping (PCM) MRI in a prototype hybrid scanner. Later, Andersen et al.^{19,20} performed simultaneous ¹⁵O-H₂O PET and ASL MRI measurements in newborn piglets, and in non-sedated newborn infants. Fan et al.¹⁷ compared rCBF in rest and after acetazolamide (ACZ) in patients with Moya-Moya disease, but as arterial blood sampling required for quantification of ¹⁵O-H₂O PET was not performed, only relative rCBF was compared. Lastly, Okazawa et al.²¹ performed simultaneous ¹⁵O-H₂O PET and ASL MRI measurements in resting state, but in the absence of arterial blood samples for quantification, an image-derived input function (IDIF) method was used to assess the input function. Fully quantitative ASL needs to be validated with fully quantitative ¹⁵O-H₂O PET in different perfusion states if assessment of physiologic changes, such as the cerebrovascular reactivity, is of interest.²²

The aim of this study was to compare multiple paired fully quantitative and simultaneous ASL MRI and ¹⁵O-H₂O PET measurements of rCBF by repetitive tracer injections in the resting state and during hypo- and hyper-perfusion in healthy young volunteers using a hybrid PET/MRI scanner.

Material and methods

Fourteen healthy young males (mean age 23.9 ± 2 years, range 21–28 years) were enrolled in the study. Inclusion criteria were: healthy males between 18 and

35 years old. Exclusion criteria were: contraindications to MRI or arterial cannulation, a medical history of prior or current neurological or psychiatric disease, or severe head trauma.

The study was approved by the Danish National Committee of Health Research Ethics (H-16023156) and was conducted according to the Declaration of Helsinki II. Written informed consent was obtained from all participants.

Experimental setup

Details of the experimental setup have been published previously along with results of comparative global CBF measurements by phase contrast MRI and ¹⁵O-H₂O PET.²³ In short, subjects were scanned twice in resting state, twice during hyperventilation (24 respirations/min) and twice after ACZ (minimum 20 min after intravenous administration of ACZ 15–20 mg/kg, Diamox, Mercury Pharmaceuticals, London, UK) in the mentioned order. Each scan consisted of a simultaneous ¹⁵O-H₂O PET and ASL MRI measurement. All PET and MRI imaging were obtained on a 3T Siemens Biograph mMR hybrid PET/MRI system (Siemens Healthcare, Erlangen Germany) within a single scanning session lasting approximately 2.5 h (see Supplementary Material S1).

The PET/MRI experiment was followed by a low dose CT (120 kV, 30 mAs, 5-mm slice width), performed in a PET/CT scanner (Siemens Biograph, Siemens, Erlangen, Germany), used for attenuation correction of the PET images.²⁴

Continuous arterial blood sampling was obtained from a catheter placed in the radial artery of the non-dominant hand. Radiotracer and ACZ were administered through a catheter placed in the median cubital vein of the contralateral forearm. Arterial blood samples for blood gases, pH, and hematocrit were obtained 4 min after the initiation of the PET measurement, approximately half way through the ASL acquisition, and were analyzed in a Radiometer ABL800 Flex system (Radiometer, Copenhagen, Denmark).

Magnetic resonance imaging

A 16-channel mMR head and neck coil designed by the vendor to minimize attenuation of the PET signal was used for all MRI measurements.

Structural imaging

A 3D T1-weighted magnetization prepared rapid acquisition gradient echo (T1-MPRAGE) was obtained prior to the first CBF measurement with the following

acquisition parameters: repetition time (TR) 1900 ms, echo time (TE) 2.44 ms, flip angle 9°, matrix 256 × 256, voxel size 1.0 × 1.0 × 1.0 mm³, GRAPPA acceleration factor 2.

T1-weighted images were segmented using Freesurfer (version 6.0, <https://surfer.nmr.mgh.harvard.edu/>) to obtain a whole brain tissue mask including cerebral hemispheres and cerebellum (excluding the ventricular system), both gray and white matter (with a 4 mm erosion to prevent spill-in from gray matter) masks, and eight regional gray matter masks (frontal, parietal, temporal and occipital lobes, cingulate, cerebellum, insula and subcortical gray matter (thalamus and basal ganglia) derived from the Desikan-Killiany Atlas template.²⁵ The masks were applied to ASL MRI and ¹⁵O-H₂O PET CBF parametric maps, previously co-registered to T1-MPRAGE, to obtain gCBF and rCBF from different regions (Supplementary Material, S2).

ASL

A 2D pseudo continuous ASL (PCASL) was chosen for its high signal-to-noise ratio. To obtain multi post-labeling delay (multi-PLD) data, the sequence was repeated at different PLDs. The labeling plane was placed across the neck 9 cm beneath the center of the imaging slab and the labeling duration was 1800 ms. The acquisition parameters were: 21 slices, TE 12 ms, voxel size 4.0 × 4.0 × 6.0 mm, FoV 256 × 256 mm, TR was adjusted for each PLD in order to keep the scanning time as short as possible. The different PLDs were set at 200, 500, 800, 1100, 1400, 1700 and 2000 ms, acquired in ascending order. Six pairs of labeled-control images were acquired in each PLD. After each ASL scan, a single equilibrium magnetization scan (M0) was acquired with the same parameters as the previously described ASL images except for a 10,000 ms TR. Total scanning time was 7 min.

ASL images were quantified using BASIL in FSL (FMRIB software library, www.fmrib.ox.ac.uk) with the full quantitative modelling described by Buxton.^{26,27} T1 relaxation time was corrected for individual hematocrit, calculated as the average from all the arterial blood samples from each subject.²⁸ The model fitted also the macrovascular compartment.²⁹ The initial prior of bolus arrival time was adjusted for the different perfusion states at 1.5 s, 1.3 s and 1.1 s for hypo-, resting- and hyper perfusion, respectively, to account for the known changes in blood velocity.²³ ASL data were registered to the T1-MPRAGE scan using the higher contrast of the M0 scan. A global arterial M0 value was calculated from a cerebrospinal fluid (CSF) mask in the ventricles and it was adjusted for the proton density of the CSF.

PET

For each PET scan, approximately 500 MBq of ¹⁵O-H₂O produced in an online system (Automatic Water Injection System, Scansys Laboratorieteknik, Værløse, Denmark) were manually injected as a bolus in the median cubital vein. Emission scans were started at the time of the radiotracer injection and recorded in list mode for 4 min. At least 10 min passed between PET measurements to allow for tracer decay.

PET images were reconstructed into 18 × 5 s, 9 × 10 s, 4 × 15 s frames using 3D-ordered subset expectation maximum (3D OSEM), 4 iterations 21 subsets, 128 × 128 matrix with voxel dimension 2 × 2 × 2 mm and 2 mm Gaussian filter. Attenuation correction was performed using μ -maps generated with a separately acquired low-dose CT scan as previously described.²⁴

Activity in the arterial blood was sampled at 1 Hz during the scans using an automatic blood sampling system (Swisstrace, Zürich, Switzerland) set to draw 8 mL/min. Flow rate, material, length (50 cm) and diameter (1 mm) of the arterial line were identical to the current clinical and research setup on our brain-dedicated PET scanner. The sampling system clock was synchronized to the scanner acquisition clock for accurate decay correction of the data. The scanner and the blood sampling system were cross-calibrated periodically and no significant variation in the calibration factor during the study period was found. Blood sampling was started approximately 90 s prior to the radiotracer injection and it was stopped 4 min after injection.

Parametric images were generated with the software PMOD 3.304 (PMOD Technologies, Zürich, Switzerland) using a one-tissue two-compartment model with correction for arterial blood volume.^{30,31} The 190 s following tracer injection of the arterial input curves were fitted into the model correcting for delay and dispersion with an exponential kernel.³² The arterial input curves were initially corrected for dead-time and decay. CBF is reported as the unidirectional clearance of tracer from the blood to the tissue (K1) assuming full extraction of water.

Statistics

All images were post-processed using an in-house developed program based on FSL (<https://fsl.fmrib.ox.ac.uk/fsl/fslwiki>) tools. ASL-CBF images were smoothed with a 3 mm full-width half maximum Gaussian filter optimized at a group level to approximately match the PET resolution.

ASL MRI and PET images were rigidly coregistered to each subject's T1-MPRAGE using FSL FLIRT³³

and the different T1-MPRAGE-based masks were applied to obtain global and regional CBF.

To perform the voxel-wise comparison, individual T1-MPRAGE images were warped into the Montreal Neurological Institute (MNI-152) space using FSL FNIRT,³⁴ and the transformation was applied to the PET and ASL CBF images. The PET and ASL CBF images were then resliced and registered to the T1-MPRAGE data set. The voxel-wise between-technique statistics was performed using a permutation-based paired T-test (randomize FSL) with 5000 permutations. The p -value was controlled for multiple comparisons using family-wise error rate.³⁵

To calculate inter-state CBF differences, only values from subjects with combined measurements in two states (post-ACZ and rest, and/or hyperventilation and rest) were included. Absolute inter-state differences were defined as the difference between each non-resting measurement (post-ACZ or in hyperventilation) and the average of the two resting measurements as follows

$$\Delta_{abs}CBF = CBF_{meas} - (CBF_{R1} + CBF_{R2})/2$$

where the subscript *meas* refers to the individual measurements in hyperventilation or post-ACZ. Relative interstate changes were defined as the absolute interstate changes over the average of the resting state measurements

$$\Delta_{rel}CBF = \frac{\Delta_{abs}CBF}{(CBF_{R1} + CBF_{R2})/2} 100 \%$$

The vascular reactivity to P_aCO_2 ($CBFR_{CO_2}$) was calculated as the relative interstate change per absolute change in P_aCO_2 as follows

$$CBFR_{CO_2} = \Delta_{rel}CBF \frac{1}{P_aCO_2HV - P_aCO_2R}$$

Average differences between states and modalities were investigated using a paired t-test. The reactivity maps (Figure 4) were calculated at a voxel level using the same equations.

The correlations between PET- and ASL-CBF measurements across all subjects were investigated with a two-level linear mixed model in order to take into account that multiple measurements were performed in each subject. ASL-MRI CBF was the dependent variable, and ^{15}O -H₂O PET CBF was entered as fixed effect, subject (μ , level 2) as random effect, and replicate measurement as residual (ε , level 1)

$$CBF_{ASL} = \beta_0 + \beta_1.CBF_{PET} + \mu + \varepsilon$$

Identical models were analyzed for each state separately and for inter-state differences. Correlation coefficients (R^2 values) for all states combined, and for each state were calculated by comparing the sum of variance components in similar two-level variance component models with and without fixed effects.³⁶ Inter- and intrasubject variability (coefficient of variation) was calculated for each state as the standard deviations of the random and residual effects, respectively, in the same model divided by the population mean.

A two-sided $p < 0.05$ was considered statistically significant for all statistical tests performed.

Results

Four scanning sessions were terminated prematurely either as a decision of the volunteer ($n = 1$) or due to arterial line clotting ($n = 3$) and two sessions were shortened due to time constraints. Finally, a single outlying resting state measurement was excluded as the ^{15}O -H₂O PET CBF value was more than three standard deviations from the population mean. In total, 63 paired and simultaneous ^{15}O -H₂O PET and ASL MRI CBF measurements were available for analysis in 14 subjects; 26 measurements in all 14 subjects in resting state, 18 measurements in 10 subjects during hyperventilation and 19 measurements in 10 subjects after ACZ.

Physiological measurements in the three different states are described in the Supplementary Material S3. In short, hyperventilation significantly decreased P_aCO_2 and increased heart rate, pH and P_aO_2 ; additionally, a reduction of 0.6 kPa in the average P_aCO_2 in the second measurement compared to the first was observed. After the administration of ACZ, a small, but significant decrease in P_aCO_2 was observed along with a slight, but non-significant, increase in the respiratory rate.

The ranges of fitted delay and dispersion values of the ^{15}O -H₂O input function were 9–15 s and 5–6 s, respectively, comparable to those we obtain using our research setup on a brain-dedicated PET scanner.³⁷

Examples of CBF maps from a single subject obtained by ^{15}O -H₂O PET and ASL MRI in each state together with T1-MPRAGE can be found in Supplementary Material S4.

Global CBF

Averaged values of global, white and gray matter CBF assessed by ASL MRI and ^{15}O -H₂O PET in the three different perfusion states and the average absolute and relative differences between them are summarized in Table 1. No significant differences were found between the averaged global, gray or white matter CBF, or in the average absolute or relative perfusion changes

Table 1. Averaged global, gray matter and white matter cerebral blood flow (ml/100 g/min) assessed by ^{15}O -H $_2\text{O}$ PET and ASL MRI.

	Hyperventilation ($n = 26$)		Rest ($n = 18$)		After-acetazolamide ($n = 19$)	
	PET	ASL	PET	ASL	PET	ASL
gCBF (mL/100 g/min)	24.5 ± 5.1	23.4 ± 4.8	40.0 ± 6.5	40.6 ± 4.1	59.0 ± 10.4	61.7 ± 10.0
Δ_{abs} gCBF (mL/100 g/min)	-14.5 ± 3.1	-17.0 ± 5.1	-	-	19.7 ± 9.1	20.1 ± 7.7
Δ_{rel} gCBF (%)	-37.3 ± 7.3	-41.9 ± 11.7	-	-	51.4 ± 24.4	48.0 ± 17.2
Intra-subject variability (%) ^a	7.8	14.9	7.1	5.1	7.3	6.0
Inter-subject variability (%) ^a	20.6	14.9	14.7	8.6	16.2	15.2
GM CBF (mL/100 g/min)	27.5 ± 5.8	26.0 ± 5.6	44.8 ± 7.6	44.6 ± 4.5	66.7 ± 12.0	67.8 ± 10.4
Δ_{abs} GM CBF (mL/100 g/min)	-16.3 ± 3.7	-18.7 ± 5.7	-	-	22.5 ± 10.3	21.9 ± 8.1
Δ_{rel} GM CBF (%)	-37.4 ± 7.3	-41.7 ± 12.4	-	-	52.4 ± 24.5	47.5 ± 16.7
WM CBF (mL/100 g/min)	9.7 ± 1.9	9.5 ± 3.7	15.9 ± 2.7	15.4 ± 4.4	21.9 ± 3.7	21.8 ± 6.1
Δ_{abs} WM CBF (mL/100 g/min)	-5.5 ± 1.6	-5.7 ± 3.7	-	-	6.5 ± 3.6	5.9 ± 4.4
Δ_{rel} WM CBF (%)	-36.0 ± 8.5	-36.7 ± 19.2	-	-	43.9 ± 24.8	39.2 ± 34.1

Note: All values are the average ± standard deviation. n indicates number of observations. The change is calculated as the difference between the average CBF in resting state and individual measurements in hyperventilation or after acetazolamide. Only subjects with measurements in at least two states contribute the calculation of CBF changes. No significant differences between the two techniques in any of the states or regions, or in the assessment of relative or absolute changes between states were found.

ASL: arterial spin labeling; PET: ^{15}O -H $_2\text{O}$ positron emission tomography; CBF: cerebral blood flow; WM: White matter; GM: Gray matter; Δ_{abs} : absolute changes; Δ_{rel} : relative changes.

^aInter and intrasubject variability is calculated as the respective standard deviations from a variance component model divided by the population mean.

Table 2. Correlation between CBF measurements and cerebral reactivity measured by ASL and PET.

	Whole brain			Gray matter			White matter		
	slope [95% CI]	R ²	p-value	slope [95% CI]	R ²	p-value	slope [95% CI]	R ²	p-value
Absolute CBF									
All states	1.01 [0.92–1.10]	0.82	<0.001	0.96 [0.87–1.05]	0.81	<0.001	0.88 [0.70–1.06]	0.51	<0.001
Rest	0.26 [0.03–0.49]	0.05	0.030	0.22 [0.04–0.39]	0.10	0.021	0.54 [0.14–0.95]	0.05	0.056
HV	0.73 [0.32–1.15]	0.47	0.003	0.66 [0.25–1.07]	0.39	0.005	0.04 [-0.80–0.89]	0.01	0.912
Post-ACZ	0.55 [0.44–0.66]	0.37	<0.001	0.53 [0.44–0.62]	0.34	<0.001	0.30 [-0.56–1.17]	0.13	0.448
Absolute reactivity									
HV – rest	0.43 [-0.41–1.28]	0.12	0.271	0.07 [-0.47–0.61]	0.00	0.778	0.32 [-0.70–0.76]	0.02	0.929
Post-ACZ – rest	0.49 [0.32–0.66]	0.26	<0.001	0.49 [0.33–0.65]	0.23	<0.001	-0.05 [-0.67–0.56]	0.01	0.848
Relative reactivity									
HV – rest	0.80 [0.03–1.58]	0.04	0.043	0.62 [-0.10–1.33]	0.11	0.083	-0.10 [-1.03–0.83]	0.00	0.809
Post-ACZ – rest	0.40 [0.18–0.63]	0.2	0.003	0.10 [0.18–0.63]	0.19	0.003	-0.34 [-1.04–0.35]	0.00	0.291

Note: Slope and R² are derived from the two-level variance component model (see Statistics). Changes are calculated as absolute and relative change from the average of the two resting measurements to each subsequent measurement. HV: hyperventilation; Post-ACZ: post acetazolamide.

between the different states between ASL MRI and ^{15}O -H $_2\text{O}$ PET. Intersubject and intrasubject variability for ^{15}O -H $_2\text{O}$ PET and ASL MRI gCBF measurements is also shown in Table 1.

Overall, a highly significant positive correlation of ASL MRI with ^{15}O -H $_2\text{O}$ PET across all states was observed in the measurements of global and gray and white matter perfusion (Table 2, Figure 1 and Supplementary Material S5). Within each state, the correlation between methods was generally poor, but

statistically significant for global and gray matter CBF. The estimate of the regression slope in each state tended to be lower than the overall estimate.

Voxel- and VOI-wise analysis

Averaged CBF maps assessed by ^{15}O -H $_2\text{O}$ PET and ASL MRI in each state and the statistical significant differences between the two techniques are shown in Figure 2. The images from the two techniques show

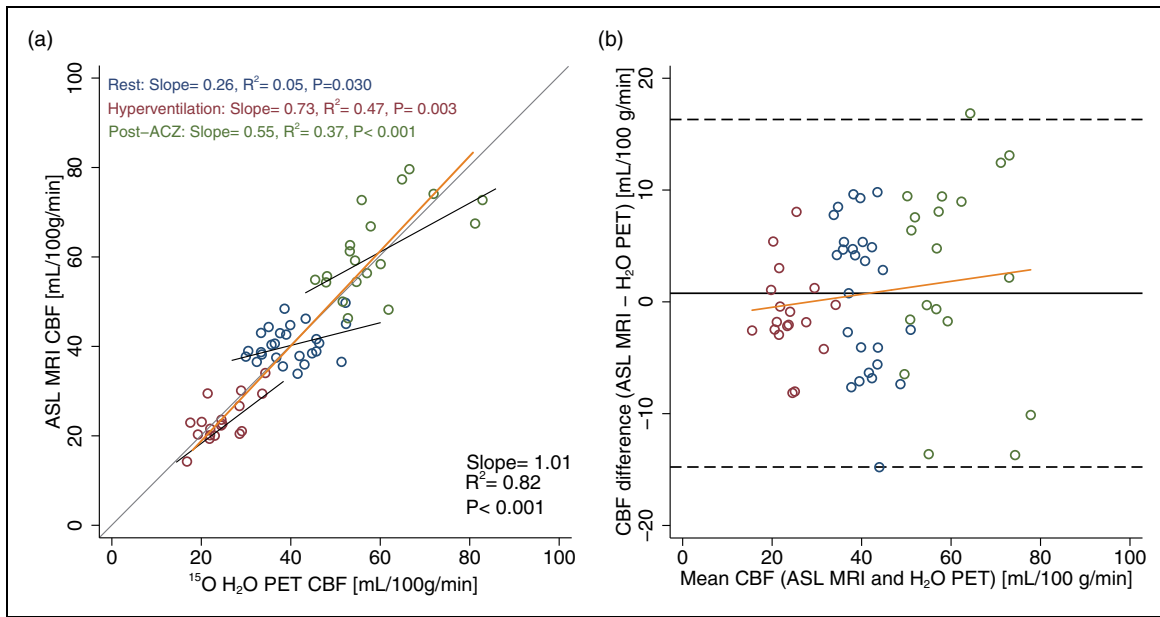


Figure 1. Correlation of gCBF measurements by ¹⁵O-H₂O PET and ASL MRI.

Scatter plot of global cerebral blood flow (gCBF) measured by ¹⁵O-H₂O PET and ASL MRI (a) and Bland-Altman plot showing the difference between the two methods against mean of the methods (b). In red, measurements during hyperventilation, in blue measurements in rest and in green measurements after acetazolamide. Orange line shows the modelled linear fit across all states and black lines the linear fit in each state from the model. In the scatter plots, grey line indicates the line of identity and in the Bland-Altman plots, solid black line indicates the average of the differences (bias) and the dashed lines the upper and lower limits of agreement (bias ± 2 SD).

Table 3. Regional absolute CBF assessed by ¹⁵O-H₂O PET and ASL MRI.

	Hyperventilation		Rest		Post-acetazolamide	
	PET	ASL	PET	ASL	PET	ASL
Frontal lobe	29.0 ± 6.1	26.3 ± 5.5 ^a	47.3 ± 8.3	44.2 ± 4.6	69.4 ± 17.7	66.6 ± 8.7
Parietal lobe	27.1 ± 5.7	26.7 ± 7.9	43.2 ± 7.7	46.5 ± 5.4	65.0 ± 11.8	71.0 ± 11.4
Temporal lobe	24.9 ± 5.3	23.2 ± 4.6	41.3 ± 6.9	40.6 ± 4.8	61.8 ± 10.9	60.3 ± 10.4
Occipital lobe	28.4 ± 6.7	23.9 ± 7.0 ^a	43.1 ± 7.8	42.9 ± 7.4	67.1 ± 13.7	71.0 ± 17.1
Cingulate	28.5 ± 6.5	35.8 ± 7.8 ^a	49.6 ± 8.9	57.6 ± 7.4 ^a	72.5 ± 13.4	89.8 ± 12.6 ^a
Cerebellum	25.5 ± 5.1	19.5 ± 5.2 ^a	43.4 ± 6.3	39.3 ± 6.2 ^a	66.1 ± 13.6	65.7 ± 16.4
Insula	28.6 ± 5.9	32.4 ± 5.1 ^a	47.9 ± 8.4	54.2 ± 5.5 ^a	69.0 ± 12.8	77.5 ± 10.2 ^a
Subcortical GM	29.0 ± 5.6	27.7 ± 5.1	47.1 ± 7.6	44.8 ± 5.4	69.1 ± 13.9	69.2 ± 10.6

Note: CBF in mL/100 g/min. Values are displayed as average CBF ± SD.

^aSignificant differences ($p < 0.05$) between the two techniques. Subcortical GM = thalamus and basal ganglia

an overall strong resemblance. However, at rest, ASL MRI yielded significantly lower perfusion than ¹⁵O-H₂O PET in the inferior temporal cortex, in the orbitofrontal cortex and in the cerebellum, whereas it yielded higher perfusion in the cingulate and in highly vascularized structures, e.g. insula. During hyperventilation, the aforementioned findings were reduced in extension and magnitude, but the ASL MRI images further showed significantly lower perfusion in the

occipital lobe and in the prefrontal region. The findings of the voxel-wise analysis were confirmed in the VOI-based analysis (Table 3). Averaged maps for arterial transit times (ATT) in the different perfusion states obtained with ASL MRI are shown in Supplementary Material S6.

Across regions, the slope of the regression line between the two techniques ranged from 0.87 to 1.14 with an R² above 0.76 in all cases. Scatter and

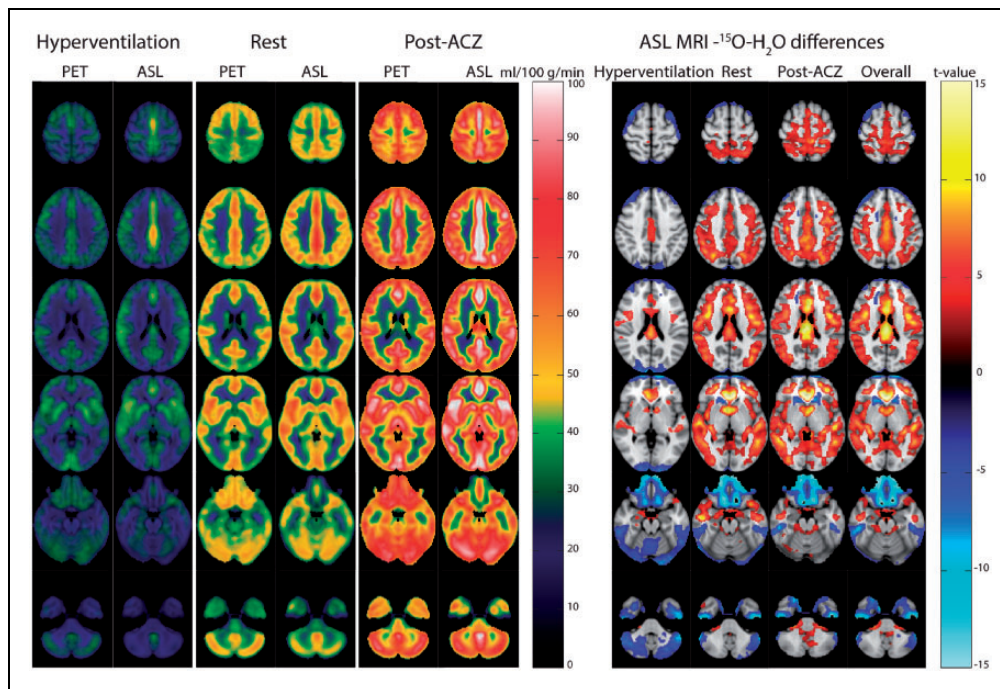


Figure 2. Average ASL and PET CBF images in different perfusion states and differences between techniques. Average $^{15}\text{O-H}_2\text{O}$ PET and ASL MRI perfusion measurements in the different perfusion states. The six columns on the left show average MRI ASL and $^{15}\text{O-H}_2\text{O}$ PET images during hyperventilation, in resting state and after acetazolamide. The four right columns show significant differences between the two techniques in each state and in all states combined. The t-value color scale is thresholded at a corrected P -value < 0.05 to show only the significantly different regions. In red-yellow ASL MRI $> ^{15}\text{O-H}_2\text{O}$ PET and in blue ASL $< ^{15}\text{O-H}_2\text{O}$ PET.

Bland–Altman plots for individual regions are provided in Supplementary Material S7.

Reactivity

The correlation of ASL MRI with $^{15}\text{O-H}_2\text{O}$ PET for quantification of absolute gCBF changes was weak and only statistically significant for post-ACZ changes. The correlation of relative gCBF-changes was slightly poorer, but significant for both ACZ and hyperventilation-induced changes. The correlation was in general stronger for post-ACZ changes compared to hyperventilation-induced changes (Table 2 and Figure 3). The vascular CO_2 reactivity during hyperventilation assessed by ASL MRI and $^{15}\text{O-H}_2\text{O}$ PET was positively correlated (Figure 3), and the average reactivities were not different (20.5 ± 1.7 and $18.6 \pm 1.4\%$ per kPa CO_2 for ASL MRI and $^{15}\text{O-H}_2\text{O}$ PET respectively, $p = 0.23$).

Figure 4 and Supplementary Material S8 show the method specific regional cerebrovascular reactivity. There was a larger absolute reactivity measured by ASL MRI in cortical areas compared to $^{15}\text{O-H}_2\text{O}$ PET. The VOI-based analysis confirmed these results in the parietal lobe, occipital lobe and in the insula for hyperventilation-induced absolute changes, and in the

cingulate for the ACZ-induced absolute changes. The relative reactivity parametric images were, in general, more homogeneous across all brain regions. Although the reactivity seemed to be larger for ASL MRI in the occipital lobes and cerebellum both for the ACZ- and hyperventilation-induced changes, they were only significant in the latter.

Discussion

The most important contribution of single scan session simultaneous PET and MRI imaging is achieving the best possible matching of physiological parameters known to influence CBF, e.g. arterial blood gases, pH, hemoglobin, caffeine levels, and sensitivity to ACZ.^{19,20} The present study is unique by obtaining 63 simultaneous and fully quantitative paired ASL MRI and $^{15}\text{O-H}_2\text{O}$ PET gCBF measurements with arterial blood sampling in healthy volunteers across different perfusion states in a single imaging session using a hybrid PET/MRI system. The number of observations by far exceeds those obtained in any single study in the existing literature comparing simultaneous ASL MRI CBF and $^{15}\text{O-H}_2\text{O}$ PET measurements with arterial blood sampling (all with ≤ 10 paired measurements),⁸

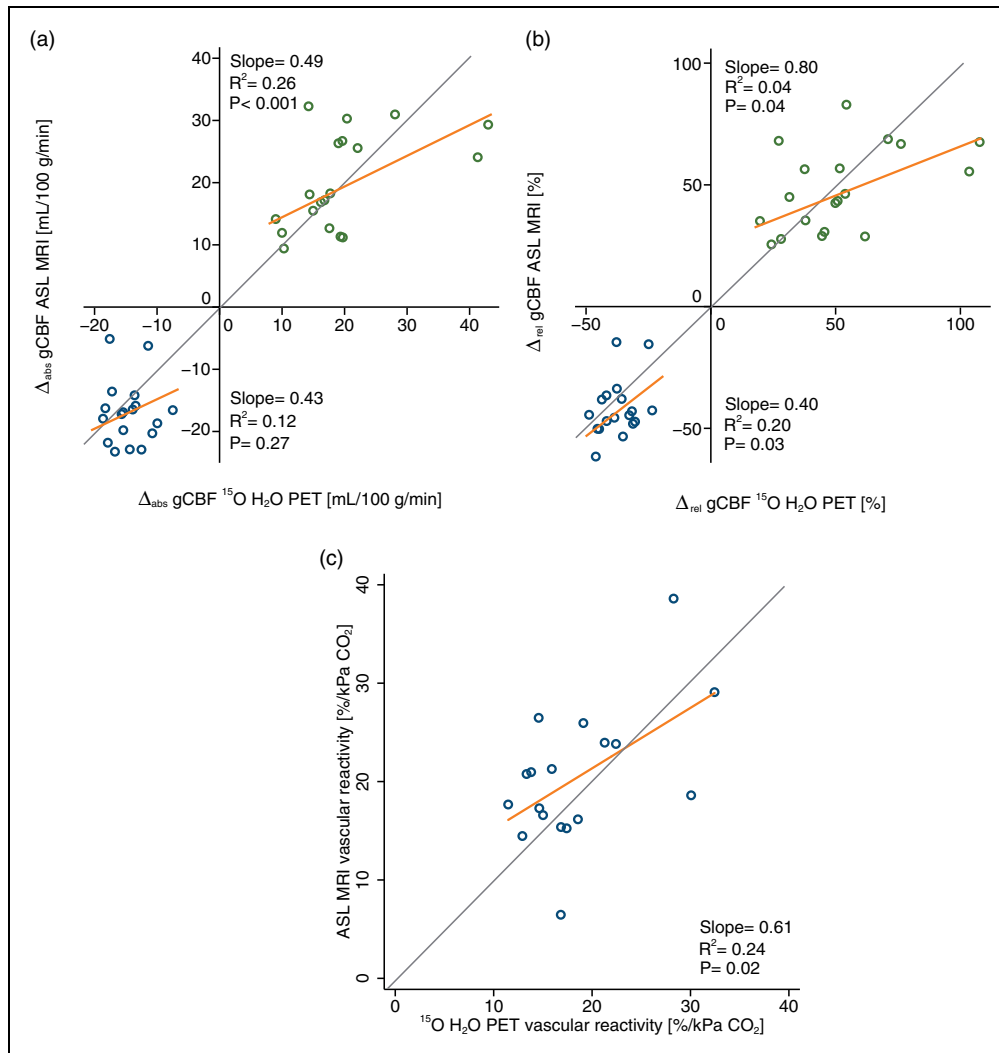


Figure 3. Global CBF reactivity. Scatter plots of (a) absolute (Δ_{abs} gCBF) and (b) relative (Δ_{rel} gCBF) between-state changes in global cerebral blood flow measured by ^{15}O -H₂O PET and ASL MRI, and of (c) relative gCBF change per % change of $P_a\text{CO}_2$ between hyperventilation and resting state. In blue, gCBF changes between hyperventilation and resting state and in green, changes between resting state and after the administration of acetazolamide. Orange line shows the linear fit from the model and the grey line indicates the line of identity.

and thus provides the best available data for assessing the accuracy of quantitative ASL MRI against an accepted reference technique.

The study shows a strong correlation between the ASL MRI and ^{15}O -H₂O PET gCBF over a wide range of perfusion values confirming the capability of ASL MRI to provide quantitative CBF measurements, also at lowered and increased perfusion. However, we also found a relatively poor agreement with regard to quantitation of resting gCBF and gCBF changes.

The average gCBF in resting state measured by ASL MRI (40.6 ± 4.1 mL/100 g/min) and by ^{15}O -H₂O PET (40.0 ± 6.5 mL/100 g/min) was not significantly different. Both techniques yielded slightly lower values compared to the generally accepted text book values of

resting gCBF around 46–50 mL/100 g/min.^{39,40} They are, however, in good agreement with those reported previously by other authors using the same techniques,⁹ as are gray and white matter CBF values,^{10,41} supporting the correct implementation of the techniques. The absolute and relative gCBF increase after the administration of ACZ measured by ASL MRI and by ^{15}O -H₂O PET is also in good agreement with published studies.^{42–44}

Two previous publications have studied fully quantitative PET and PCASL in a comparable population and using similar techniques, although performing measurements on different study days and only acquired single PLD ASL data. Van Golen et al. compared single resting measurements and found, similar to

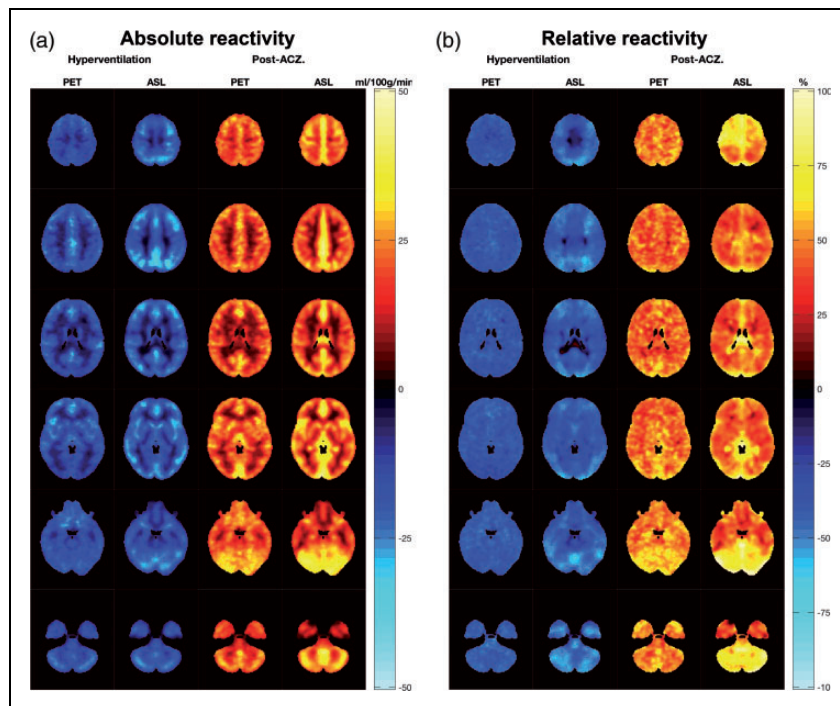


Figure 4. Method specific regional cerebrovascular reactivity. Absolute (a) and relative (b) average reactivity maps between hyperventilation and resting state (blue, for CBF decrease) and post-ACZ and resting state (in red and yellow, for CBF increase) measured by $^{15}\text{O}\text{-H}_2\text{O}$ PET and ASL MRI.

our study, a relatively poor correlation of resting state measurements with a non-significant, although slightly higher, correlation coefficient between gCBF resting measurements ($R^2=0.13$ vs. 0.05 in our study) with a very similar slope of the regression line (0.27 vs. 0.26 in our study).³⁷ Heijtel et al. performed multiple measurements both in rest and during hypercapnia on both study days and found similar to the present study that the correlation improved greatly when including all measurements from both conditions, and found similar to our study a linear regression line close to line of identity (slope 1.0 and $R^2=0.47$ vs slope 1.01 and $R^2=0.82$ in the present study).¹⁰

Method-imprecision is a possible cause of both the weak correlation between methods and also the lower slope of the regression line (due to attenuation bias) in individual states compared to the overall correlation, and amplified when studying a homogenous population with relatively low interindividual variability, in particular in rest. The greater inter-subject variability of the $^{15}\text{O}\text{-H}_2\text{O}$ PET compared to ASL MRI (Table 1) in resting state may further contribute to the lower slope in rest. Intra-subject variability of both methods is similar to what has been reported previously.^{14,37} Based on the estimated intra- and inter-subject variability in resting state, the expected attenuation factors for $^{15}\text{O}\text{-H}_2\text{O}$ PET and ASL were 0.81 and 0.74 , respectively. The expected correlation coefficient (R^2) between

techniques in resting state, accounting for intra- and inter-subject variability was therefore 0.60 . Considering the differences between the observed (0.05) and expected (0.60) resting R^2 , we performed a post hoc power calculation. The power for detecting a significant correlation of 0.77 ($R^2=0.60$) with a sample size of 14 is 0.95 (two-sided $p < 0.05$). We can conclude therefore that the poor correlation was not a consequence of an underpowered study, but rather truly poor method correlation at rest. Several factors could introduce subject or measurement specific rCBF quantification errors in both techniques, in particular parameters that are estimated or assumed from literature values (e.g. for ASL labelling efficiency, partition coefficient, and T1 of blood and tissue) or factors that may influence the single measurements (e.g. for ASL head motion, and for PET the quality of the AIF measurement) that would mainly influence smaller within state differences at rest. The better correlation between the two techniques in hypo- and hyperperfusion is most likely explained by the broader range of the gCBF measurements, reducing the impact of the method-imprecision.

The perfusion distribution images obtained with the two techniques showed good resemblance. The regional differences between the two techniques visualized in Figure 2 can be explained by well-known methodological ASL MRI limitations. The lower ASL MRI

rCBF in the orbitofrontal cortex, the inferior temporal lobes, cerebellum and the cranial base is related to susceptibility-induced artifacts affecting areas close to air and bone interface when using an echo-planar read-out,¹⁰ while the higher rCBF in highly vascularized regions and in the cingulate probably corresponds to residual vascular signal that cannot be estimated in the kinetic model due to the delayed read out.^{9,10} The vascular signal could have been lowered with the application of vascular crushing at the expense of a prolonged acquisition time.³⁸ The change in the distribution of the ASL MRI and ¹⁵O-H₂O PET perfusion differences during hyperventilation is probably caused by better identification of the macrovascular compartment as a consequence of the higher signal in the vessels due to the longer arterial transit time. We did not observe hypoperfusion in the basal ganglia on ASL MRI compared to ¹⁵O-H₂O PET as previously described by Heijtel et al.¹⁰ probably because of methodological difference in the ASL sequence implementation and post-processing, such as the use of a multi versus fixed post-labelling delay approaches.

Quantification of cerebrovascular reactivity is an important application of quantitative CBF measurements and, in particular, in the assessment of vascular reserve by the ACZ challenge.⁴⁶ The average gCBF increase assessed by ASL MRI and ¹⁵O-H₂O PET during the ACZ challenge was not different. The correlation between the assessment of gCBF changes was significant, but relatively weak ($R^2 = 0.26$ and $R^2 = 0.20$ for absolute and relative reactivity, respectively), with a regression line slope just below 0.5, probably as a consequence of the attenuation bias due to method imprecision. Average CO₂ reactivity measured by ¹⁵O-H₂O PET and ASL MRI were not different and were both within the range of previously published results,⁴⁷ and also the correlation between methods was significant although modest ($R^2 = 0.29$). The high absolute reactivity in the cingulate between hyperperfusion (achieved by hypercapnia) and resting state observed in ASL MRI images was also observed by Zhou et al.⁴⁸ (cerebellum was not shown). In the study Heijtel et al.,¹⁰ higher relative reactivity was found in the lower and posterior parts of the brain (cerebellum was not studied) in ASL MRI compared to ¹⁵O-H₂O PET. Hence, caution is advised when using PCASL for reactivity studies, and further evaluation is needed. The single PLD PCASL approach applied in most previous studies requires a careful and accurate selection of the PLD to be longer than the longest regional ATT in order to avoid signal loss.³⁸ So although a single PLD scan may be a valid approach in many cases, clinical use may be compromised by artificially induced low rCBF in brain regions with unusually long ATT caused by old age or pathology. The multi PLD

PCASL approach used in this study should provide a more robust rCBF estimate by modelling a wider range of ATTs,³⁸ allowing for a single scanning protocol suitable for all perfusion states, although at the expense of poorer SNR and longer acquisition time. The greater intra-subject variability of ASL MRI compared to PET in hyperventilation might reflect a combination of a greater sensitivity to long ATT from ASL, even with the multi PLD approach used, and to head motion.

Using ¹⁵O-H₂O PET, CBF might be underestimated, especially during hyperperfusion, due to the flow-dependent limitation on water extraction across the blood-brain barrier (approximately 0.85 at resting CBF values) when quantifying CBF from ¹⁵O-H₂O PET using the unidirectional clearance rate constant, K_1 , of a one-tissue two-compartment model.⁴⁵ However, as the signal in ASL MRI and ¹⁵O-H₂O PET CBF reflects the physiological properties of water transport in the brain, the correlation is retained across states, as opposed to other MRI techniques to measure CBF, such as PCM MRI.³⁷

One limitation of this study is the inclusion of a relatively homogenous and small study population of young males only, and the relatively high number of incomplete studies as a consequence of the complexity of the setup. Young males were expected to have larger vessels making arterial cannulation easier and more optimal for vessel related measurements,²³ and were, based on our experiences from previous studies, expected to better comply with the stressful experimental setup compared to aged subjects. Including a population with a larger expected biological variability may potentially have improved method correlation in resting measurements. This limitation is compensated for by performing multiple paired measurements in different perfusion states using repeated tracer injection. The premature abortion of 3/14 studies due to arterial line clotting can be explained by a suboptimal wrist position because of physical limitations when using a PET/MRI scanner. This supports the perception that an alternative approach to ¹⁵O-H₂O PET would be convenient, which is a justification for this study.

It has recently been suggested that the combined pharmacokinetic modelling of simultaneously acquired cerebellar rCBF by fixed PLD pASL MRI together with late phase ¹⁸F-florbetapir amyloid PET data could be a feasible strategy to substantially reduce the acquisition time from 90 to 30 min. This strategy would retain an accurate measure of the cortical binding potential free of the influence of blood flow.⁴⁹ However, our finding of a significant systematic reduction of both cerebellar rCBF and relative reactivity in ASL (Table 3 and Figure 4(b)) discourages its use as a reference region and for normalizing ASL MRI rCBF measurements in different perfusion states.⁵⁰

Even though $^{15}\text{O}\text{-H}_2\text{O}$ PET and ASL employ the same tracer and thereby are very similar with regard to tracer distribution in tissue and diffusion through the vessel wall (Crone-Renkin effect)⁵¹ and the spatial resolutions were matched, there are still subtle differences between the two techniques which potentially can explain differences when comparing results from the two methods. The models employed for $^{15}\text{O}\text{-H}_2\text{O}$ PET and ASL MRI quantification share some similarities. Both models are two-compartment one-tissue models with arterial blood volume and assume a uniform arrival of the blood at a particular voxel, an instantaneous equilibrium in the compartments and a fast and complete extraction of water from the vascular space. Regarding the arterial input function, for the PET model it is measured directly in blood, while for ASL it is assumed indirectly based on the labelling technique and assumptions of labelling efficiency. The half-life of the tracer (124 s for $^{15}\text{O}\text{-H}_2\text{O}$ and ~ 1.7 s for magnetically labelled water in a 3T MRI scanner) is accounted for in both models. The temporal resolution for two sequential whole-brain rCBF measurements using ASL MRI is 7.5 min using our setup, while it is 10 min for $^{15}\text{O}\text{-H}_2\text{O}$ PET to allow for sufficient tracer decay.

However, it is remarkable that despite many subtle, but nevertheless substantial differences between MRI and PET, very similar results between the two modalities have been obtained probably due to their relatively low impact in the final CBF calculation.

In conclusion, this study shows that this particular ASL MRI implementation and $^{15}\text{O}\text{-H}_2\text{O}$ PET rCBF measurements performed simultaneously across different perfusion states are highly correlated, but show poorer correlation within individual states, in particular in resting state measurements, and only moderate correlation in hemodynamic reactivity and with systematic differences in the regional distribution. The importance of these differences relies upon the specific context, e.g. how large errors are acceptable compared to the clinically or experimentally relevant change. In future work, this technique will be used on patients with symptomatic carotid occlusions to further investigate its robustness.

Funding

The author(s) disclosed receipt of the following financial support for the research, authorship, and/or publication of this article: Oriol Puig is supported by a training grant from the Fundación Alfonso Martín Escudero and Claes N. Ladefoged is supported by a post doc grant from the Danish Council for Independent Research (reference number: 6110-00692A).

Acknowledgements

The authors would like to thank the hard work and dedication of the nuclear medicine technologists and radiographers

Nadia Azizi, Marianne Federspiel, Jakup Poulsen and Karin Stahr; the staff of the Cyclotron and Radiochemistry Unit, Annette Ulrich, from the cardiothoracic anesthesiology department for the arterial cannulations, the Trauma Center for the assistance with the arterial blood gases analysis, and Lasse Anderberg for his help with the post-processing. We would like to acknowledge the University of Southern California's Stevens Neuroimaging and Informatics Institute and The Regents of the University of California as the sources of the Licensed Technology used. We would also like to thank The John and Birthe Meyer Foundation, who generously donated the PET/MRI scanner and the cyclotron to Copenhagen University Hospital Rigshospitalet.

Declaration of conflicting interests

The author(s) declared no potential conflicts of interest with respect to the research, authorship, and/or publication of this article.


Authors' contributions

OP, OH, UL and IL contributed to the design of the study, acquisition, analysis and interpretation of the data, and the drafting of the article. ER and HBWL contributed to the design of the study and analysis and interpretation of the data, and the drafting of the article. MBV, AEH, FLA and CNL contributed to the analysis and interpretation of the data and the drafting of the article. All authors revised critically the draft and approved the version to be published.

Supplemental material

Supplemental material for this paper can be found at the journal website: <http://journals.sagepub.com/home/jcb>

ORCID iD

Oriol Puig  <https://orcid.org/0000-0002-3510-9204>

References

1. Raichle ME, Martin WRW, Herscovitch P, et al. Brain Blood Flow Measured with Intravenous H₂¹⁵O. II. Implementation and Validation. *J Nucl Med* 1983; 24: 790–798.
2. Rostrup E, Knudsen GM, Law I, et al. The relationship between cerebral blood flow and volume in humans. *Neuroimage* 2005; 24: 1–11.
3. Powers WJ, Clarke WR, Jr RLG, et al. Extracranial-intracranial bypass surgery for stroke prevention in hemodynamic cerebral ischemia the carotid occlusion surgery study randomized trial. *JAMA* 2011; 306: 1983–1992.
4. Zhou Y, Rodgers ZB and Kuo AH. Cerebrovascular reactivity measured with arterial spin labeling and blood oxygen level dependent techniques. *Magn Reson Imaging* 2015; 33: 566–576.
5. Verfaillie SCJ, Adriaanse SM, Binnewijzend MAA, et al. Cerebral perfusion and glucose metabolism in Alzheimer's disease and frontotemporal dementia: two sides of the same coin? *Eur Radiol* 2015; 25: 3050–3059.

6. Sierra-Marcos A, Carreño M, Setoain X, et al. Accuracy of arterial spin labeling magnetic resonance imaging (MRI) perfusion in detecting the epileptogenic zone in patients with drug-resistant neocortical epilepsy: comparison with electrophysiological data, structural MRI, SISCOM and FDG-PET. *Eur J Neurol* 2016; 23: 160–167.
7. Wang DJJ, Alger JR, Qiao JX, et al. Multi-delay multi-parametric arterial spin-labeled perfusion MRI in acute ischemic stroke - Comparison with dynamic susceptibility contrast enhanced perfusion imaging. *Neuroimage Clin* 2013; 3: 1–7.
8. Zhang K, Herzog H, Mauler J, et al. Comparison of cerebral blood flow acquired by simultaneous [15O]water positron emission tomography and arterial spin labeling magnetic resonance imaging. *J Cereb blood flow Metab* 2014; 34: 1373–1380.
9. Van Golen LW, Kuijper JPA, Huisman MC, et al. Quantification of cerebral blood flow in healthy volunteers and type 1 diabetic patients: comparison of MRI arterial spin labeling and [15 O] H 2 O Positron emission tomography (PET). *J Magn Reson Imaging* 2014; 40: 1300–1309.
10. Heijtel DFR, Mutsaerts HJMM, Bakker E, et al. Accuracy and precision of pseudo-continuous arterial spin labeling perfusion during baseline and hypercapnia: a head-to-head comparison with 15O H2O positron emission tomography. *Neuroimage* 2014; 92: 182–192.
11. Qiu M, Maguire RP, Arora J, et al. Arterial transit time effects in pulsed arterial spin labeling cbf mapping: insight from a PET and MR study in normal human subjects. *Magn Reson Med* 2010; 63: 374–384.
12. Xu G, Rowley HA, Wu G, et al. Reliability and precision of pseudo-continuous arterial spin labeling perfusion MRI on 3.0 T and comparison with 15 O-water PET in elderly subjects at risk for Alzheimer's disease. *NMR Biomed* 2010; 23: 286–293.
13. Kilroy E, Apostolova L, Liu C, et al. Reliability of two-dimensional and three-dimensional pseudo-continuous arterial spin labeling perfusion mri in elderly populations: comparison with 15O-water positron emission tomography. *J Magn Reson Imaging* 2014; 39: 931–939.
14. Henriksen OM, Larsson HBW, Hansen AE, et al. Estimation of intersubject variability of cerebral blood flow measurements using MRI and positron emission tomography. *J Magn Reson Imaging* 2012; 35: 1290–1299.
15. Goetti R, Warnock G, Kuhn FP, et al. Quantitative cerebral perfusion imaging in children and young adults with moyamoya disease: comparison of arterial. *Pediatrics* 2014; May: 1022–1028.
16. Bokkers RPH, Bremmer JP, Van Berckel BNM, et al. Arterial spin labeling perfusion MRI at multiple delay times: a correlative study with H 215 O positron emission tomography in patients with symptomatic carotid artery occlusion. *J Cereb Blood Flow Metab* 2009; 30: 222–229.
17. Fan AP, Guo J, Khalighi MM, et al. Long-delay arterial spin labeling provides more accurate cerebral blood flow measurements in moyamoya patients: a simultaneous positron emission tomography/MRI study. *Stroke* 2017; 48: 2441–2449.
18. Fan AP, Jahanian H, Holdsworth SJ, et al. Comparison of cerebral blood flow measurement with [15O]-water positron emission tomography and arterial spin labeling magnetic resonance imaging: a systematic review. *J Cereb blood Flow Metab* 2016; 36: 842–861.
19. Andersen JB, Henning WS, Lindberg U, et al. Positron emission tomography / magnetic resonance hybrid scanner imaging of cerebral blood flow using 15 O-water positron emission tomography and arterial spin labeling magnetic resonance imaging in newborn piglets. *J Cereb Blood Flow Metab* 2015; 35: 1703–1710.
20. Andersen JB, Lindberg U, Olesen OV, et al. Hybrid PET/MRI imaging in healthy unselected newborn infants with quantitative rCBF measurements using 15O-water PET. *J Cereb Blood Flow Metab* 2019; 39: 782–793.
21. Okazawa H, Higashino Y, Tsujikawa T, et al. Noninvasive method for measurement of cerebral blood flow using O-15 water PET/MRI with ASL correlation. *Eur J Radiol* 2018; 105: 102–109.
22. Gao Y, Zhang J, Liu H, et al. Regional cerebral blood flow and cerebrovascular reactivity in Alzheimer's disease and vascular dementia assessed by arterial spin-labeling magnetic resonance imaging. *Curr Neurovasc Res* 2013; 10: 49–53.
23. Puig O, Vestergaard MB, Lindberg U, et al. Phase contrast mapping MRI measurements of global cerebral blood flow across different perfusion states – a direct comparison with O-H 2 O positron emission tomography using a hybrid PET / MR system. *J Cereb Blood Flow Metab*. Epub ahead of print 11 September 2018. DOI: 10.1177/0271678X18798762.
24. Andersen FL, Ladefoged CN, Beyer T, et al. Combined PET/MR imaging in neurology: MR-based attenuation correction implies a strong spatial bias when ignoring bone. *Neuroimage* 2014; 84: 206–216.
25. Desikan RS, Ségonne F, Fischl B, et al. An automated labeling system for subdividing the human cerebral cortex on MRI scans into gyral based regions of interest. *Neuroimage* 2006; 31: 968–980.
26. Chappell MA, Groves AR, Whitcher B, et al. Variational Bayesian inference for a nonlinear forward model. *IEEE Trans Signal Process* 2009; 57: 223–236.
27. Buxton RB, Frank LR, Wong EC, et al. A general kinetic model for quantitative perfusion imaging with arterial spin labeling. *Magn Reson Med* 1998; 40: 383–396.
28. Lu H, Clingman C, Golay X, et al. Determining the longitudinal relaxation time (T1) of blood at 3.0 tesla. *Magn Reson Med* 2004; 52: 679–682.
29. Chappell MA, Donahue MJ, Woolrich MW, et al. Separation of macrovascular signal in multi-inversion time arterial spin labelling MRI. *Magn Reson Med* 2010; 63: 1357–1365.
30. Ohta S, Meyer E, Fujita H, et al. Cerebral [15O] water clearance in humans determined by PET: I. Theory and normal values. *J Cereb Blood Flow Metab* 1996; 16: 765–780.
31. Fujita H, Meyer E, Reutens D, et al. Cerebral [15O] water clearance in humans determined by positron emission tomography: II. Vascular responses to vibrotactile stimulation. *J Cereb Blood Flow Metab* 1997; 17: 73–79.

32. Iida H, Kanno I, Miura S, et al. Determination of the regional brain/blood partition coefficient of water using dynamic positron emission tomography. *J Cereb Blood Flow Metab* 1989; 9: 874–885.
33. Jenkinson M, Bannister P, Brady M, et al. Improved optimization for the robust and accurate linear registration and motion correction of brain images. *Neuroimage* 2002; 17: 825–841.
34. Andersson JLR, Jenkinson M and Smith S. *Non-linear registration, aka spatial normalisation*. FMRIB Technical Report TR07JA2, 2007.
35. Winkler AM, Ridgway GR, Webster MA, et al. Permutation inference for the general linear model. *Neuroimage* 2014; 92: 381–397.
36. Snijders TAB and Bosker RJ. *Multilevel analysis: an introduction to basic and advanced multilevel modeling*. 2nd ed. Thousand Oaks, CA: SAGE, 2011.
37. Vestergaard MB, Lindberg U, Aachmann-Andersen NJ, et al. Comparison of global cerebral blood flow measured by phase-contrast mapping MRI with ^{15}O -H $_2\text{O}$ positron emission tomography. *J Magn Reson Imaging* 2017; 45: 692–699.
38. Alsop DC, Detre JA, Golay X, et al. Recommended implementation of arterial spin-labeled perfusion MRI for clinical applications: a consensus of the ISMRM perfusion study group and the European consortium for ASL in dementia. *Magn Reson Med* 2014; 116: 102–116.
39. Lassen NA. Normal average value of cerebral blood flow in younger adults is 50 ml/100 g/min. *J Cereb Blood Flow Metab* 1985; 5: 347–349.
40. Madsen PL, Holm S, Herning M, et al. Average blood-flow and oxygen-uptake in the human brain during resting wakefulness – a critical-appraisal of the kety-schmidt technique. *J Cereb Blood Flow Metab* 1993; 13: 646–655.
41. Van Osch MJP, Teeuwisse WM, Van Walderveen MAA, et al. Can arterial spin labeling detect white matter perfusion signal? *Magn Reson Med* 2009; 62: 165–173.
42. Detre J, Samuels OB, Alsop D, et al. Noninvasive magnetic resonance imaging evaluation of cerebral blood flow with acetazolamide challenge in patients with cerebrovascular stenosis. *J Magn Reson Imaging* 1999; 10: 870–875.
43. Okazawa H, Yamauchi H, Sugimoto K, et al. Effects of acetazolamide on cerebral blood flow, blood volume, and oxygen metabolism: a positron emission tomography study with healthy volunteers. *J Cereb Blood Flow Metab* 2001; 21: 1472–1479.
44. Spilt A, Van Den Boom R, Kamper AM, et al. MR assessment of cerebral vascular response: a comparison of two methods. *J Magn Reson Imaging* 2002; 16: 610–616.
45. Paulson O, Hertz M, Bolwig T, et al. Filtration and diffusion of water across the blood-brain barrier in man. *Microvasc Res* 1977; 13: 113–124.
46. Vagal AS, Leach JL, Fernandez-Ulloa M, et al. The acetazolamide challenge: techniques and applications in the evaluation of chronic cerebral ischemia. *Am J Neuroradiol* 2009; 30: 876–884.
47. Ito H, Yokoyama I, Iida H, et al. Regional differences in cerebral vascular response to P(a)CO $_2$ changes in humans measured by positron emission tomography. *J Cereb Blood Flow Metab* 2000; 20: 1264–1270.
48. Zhou Y, Rodgersl ZB and Kuo AH. Cerebrovascular reactivity measured with arterial spin labeling and blood oxygen level dependent techniques. *Magn Reson Imaging* 2015; 33: 566–576.
49. Scott CJ, Jiao J, Melbourne A, et al. Reduced acquisition time PET pharmacokinetic modelling using simultaneous ASL–MRI: proof of concept. *J Cereb Blood Flow Metab*. Epub ahead of print 5 September 2018. DOI: 10.1177/0271678X18797343.
50. Lacalle-Aurioles M, Alemán-Gómez Y, Guzmán-Devilloria JA, et al. Is the cerebellum the optimal reference region for intensity normalization of perfusion MR studies in early Alzheimer’s disease? *PLoS One* 2013; 8: 1–8.
51. Lorthois S, Duru P, Billanou I, et al. Kinetic modeling in the context of cerebral blood flow quantification by H $_2$ ^{15}O positron emission tomography: the meaning of the permeability coefficient in Renkin-Crone[U+05F3]s model revisited at capillary scale. *J Theor Biol* 2014; 353: 157–169.